Optimizing sensitivity to γ with $B^0 \to DK^+\pi^-$, $D \to K^0_S\pi^+\pi^-$ double Dalitz plot analysis

D. Craik,[1] T. Gershon,[2] and A. Poluektov[2]

[1]Massachusetts Institute of Technology, Cambridge, Massachusetts 02139, USA
[2]Department of Physics, University of Warwick, Coventry CV4 7AL, United Kingdom

(Received 21 December 2017; published 5 March 2018)

Two of the most powerful methods currently used to determine the angle γ of the CKM Unitarity Triangle exploit $B^+ \to DK^+$, $D \to K^0_S\pi^+\pi^-$ decays and $B^0 \to DK^+\pi^-$, $D \to K^+K^-$, $\pi^+\pi^-$ decays. It is possible to combine the strengths of both approaches in a "double Dalitz plot" analysis of $B^0 \to DK^+\pi^-$, $D \to K^0_S\pi^+\pi^-$ decays. The potential sensitivity of such an analysis is investigated in the light of recently published experimental information on the $B^0 \to DK^+\pi^-$ decay. The formalism is also expanded, compared to previous discussions in the literature, to allow $B^0 \to DK^+\pi^-$ with any subsequent D decay to be included.

DOI: 10.1103/PhysRevD.97.056002

I. INTRODUCTION

Within the standard model, the sole source of CP violation is the complex phase of the Cabibbo-Kobayashi-Maskawa (CKM) quark mixing matrix [1,2]. The amount of matter-antimatter asymmetry related to this source can be quantified through the area of the unitarity triangle formed from elements of the CKM quark mixing matrix [3]. The angle $\gamma \equiv \arg[-V_{ud}V^*_{ub}/(V_{cd}V^*_{cb})]$ of this triangle is a particularly important parameter, since it can be determined with negligible theoretical uncertainty [4] using methods that are reliable in the standard model and in any extensions that do not affect tree-level b hadron decays [5]. The current world average value is $\gamma = (76.2^{+4.7}_{-5.0})°$ [6], dominated by recent results from LHCb [7–11]. The uncertainty is still far from the subdegree precision that is strived for, and therefore improving the measurement of γ remains one of the main objectives of current and planned flavor physics experiments [12–14].

Numerous variations of methods to determine γ have been proposed, and a significant number have now been attempted experimentally (see reviews in Refs. [6,15]). In this work, the focus is on methods based on Dalitz plot analysis of $B^0 \to DK^+\pi^-$ decays [16,17], where the neutral D meson is reconstructed in final states to which both D^0 and $\bar{D}^0$ can decay.[1] The Dalitz plot contains resonant and nonresonant contributions, including those for $B^0 \to DK^*(892)^0$ and $B^0 \to D^*_2(2460)^-K^+$ decays. In the $B^0 \to DK^{*0}$ case,[2] the amplitudes from $b \to c$ transitions can interfere with those from $b \to u$ transitions, and CP-violating observables are related to their relative weak (i.e., CP-violating) and strong (i.e., CP-conserving) phases γ and δ_B, as well as their relative magnitude, r_B. One advantage of using neutral B meson decays to determine γ, compared to the more familiar approach with $B^+ \to DK^+$ decays [18–21], is that the value of r_B associated with $B^0 \to DK^{*0}$ transitions is expected to be larger (typical expectations are $r_B(DK^{*0}) \sim 0.3$, $r_B(DK^+) \sim 0.1$, while the latest world averages are $r_B(DK^{*0}) = 0.226^{+0.042}_{-0.045}$, $r_B(DK^+) \sim 0.105 \pm 0.005$ [6]). Another advantage of the Dalitz plot analysis approach is that interference effects between the amplitudes for DK^{*0} and contributions such as $D^*_2(2460)^-K^+$ involving $D\pi^-$ resonances, which are mediated by $b \to c$ transitions only, can be used to enhance the sensitivity and resolve ambiguities in the allowed values of γ [16].

The LHCb collaboration has recently performed the first determination of γ with $B^0 \to DK^+\pi^-$ Dalitz plot analysis, using D meson decays to K^+K^- and $\pi^+\pi^-$ [22], building on knowledge of the $B^0 \to \bar{D}^0K^+\pi^-$ Dalitz plot structure obtained in an earlier analysis (with $\bar{D}^0 \to K^+\pi^-$) [23]. The precision obtained on the parameters $x_\pm = r_B\cos(\delta_B \pm \gamma)$ and $y_\pm = r_B\sin(\delta_B \pm \gamma)$ is comparable [24] to that from analysis of $B^0 \to DK^{*0}$, $D \to K^0_S\pi^+\pi^-$ decays [25,26] selected from the same data sample. This demonstrates the potential impact of the $B^0 \to DK^+\pi^-$ Dalitz plot technique on the determination of γ. In the latter analysis a "quasi-two-body" approach is used, in which the K^{*0} resonance is treated as a stable particle and the effects of

[1]The symbol D is used to refer to a neutral charm meson that is any admixture of D^0 and $\bar{D}^0$ states.

[2]Throughout this paper the symbol K^* will be used to denote the $K^*(892)$ resonance unless explicitly stated otherwise.

other contributions in the selected region of the $DK^+\pi^-$ Dalitz plot are absorbed in hadronic parameters [27]. A further advantage of the Dalitz plot analysis is that this treatment is not necessary, and moreover the extra hadronic parameters that enter in the quasi-two-body approach can be measured.

The results of the Dalitz plot analysis [22] however suffer from two important sources of systematic uncertainty. The first is that the modeling of the suppressed and favored amplitudes in $B^0 \to DK^+\pi^-$ decays impacts the obtained results. While narrow resonances such as the $K^*(892)^0$ and $D_2^*(2460)^-$ states can be reliably described by relativistic Breit–Wigner functions, there are also broad (e.g., $K_0^*(1430)^0$ and $D_0^*(2400)^-$) and possible nonresonant contributions for which an appropriate range of alternative line shapes must be considered. The second is due to background from $\bar{B}_s^0 \to D^*K^+\pi^-$, where the soft pion or photon from $D^* \to D\pi^0$ or $D\gamma$ is not included in the reconstruction, which peaks near to the signal region. Since the favored final state for the B^0 decay is suppressed for the B_s^0 decay, and vice versa, this particularly impacts the $B^0 \to DK^+\pi^-$, $D \to K^-\pi^+$ channel (which, for this reason, was not included in the LHCb analysis [22]), but is also important for the $B^0 \to DK^+\pi^-$, $D \to K^+K^-$ and $\pi^+\pi^-$ modes. It should be noted, however, that this issue would not affect analyses performed on data samples collected using the $e^+e^- \to \Upsilon(4S) \to B\bar{B}$ process, such as those that will be available in the Belle II experiment, since there is no production of B_s^0 mesons in that case.

Both of these effects suggest that a promising way to proceed may be via model-independent double Dalitz plot analysis of the $B^0 \to DK^+\pi^-$, $D \to K_S^0\pi^+\pi^-$ decay. This method, introduced in Ref. [28], builds on ideas introduced for $B^+ \to DK^+$, $D \to K_S^0\pi^+\pi^-$ decays [29–32], where the D decay Dalitz plot is divided into bins. Each of the bins is described by hadronic parameters corresponding approximately to the average cosine or sine of the strong phase difference between the amplitudes for D^0 and $\bar{D}^0$ decays in that bin. Together with external input on the D decay hadronic parameters, as can be (and has been) obtained from $\psi(3770) \to D^0\bar{D}^0$ data [33], only the yield in each bin needs to be determined from B decay data in order to have sensitivity to γ. The key additional ingredient in the double Dalitz plot analysis is that the B decay Dalitz plot can also be binned, and that the corresponding B decay hadronic parameters can be determined from the data simultaneously with γ with no additional external information required. Additional D decays, such as $D \to K^+K^-$ and $\pi^+\pi^-$ can be included in the analysis and provide extra sensitivity, but the three-body D decay is necessary in order for the method to work. Thus, in this paper the phrase "model-independent double Dalitz plot analysis" refers to the study of $B^0 \to DK^+\pi^-$ decays with any set of D meson decays that includes $D \to K_S^0\pi^+\pi^-$.

The model-independent double Dalitz plot analysis approach not only resolves the issue of model-dependency, but also ameliorates the challenges presented by the $\bar{B}_s^0 \to D^*K^+\pi^-$ background because a detailed description of the phase-space distribution of this decay is no longer required. Instead, only the shape of the background in the $DK^+\pi^-$ invariant mass need be described. Recent results from LHCb have demonstrated how this can be achieved [9].

Consequently, it is timely to reexamine the potential of the model-independent double Dalitz plot analysis to determine γ. This allows the study of Ref. [28] to be updated, incorporating information about $B^0 \to DK^+\pi^-$ decays that is now available, and also with more realistic estimates of the yields that should be available at LHCb after the completion of LHC Run II, and with larger data samples. In addition, the previous study considered as a baseline including only the $D \to K_S^0\pi^+\pi^-$ mode together with the favored $D \to K^+\pi^-$ channel for normalization, with the impact of adding $D \to K^+K^-$ and $\pi^+\pi^-$ decays also assessed. The updated study presented here also considers inclusion of the suppressed $D \to K^-\pi^+$ decay. Indeed, the formalism set out in Sec. II allows any D decay mode to be included in the analysis. An estimate of the potential sensitivity, and its dependence on sample size, binning of the Dalitz plot, inclusion of different D decay modes and on the impact of the $\bar{B}_s^0 \to D^*K^+\pi^-$ background is presented in Sec. III. A summary concludes the paper in Sec. IV.

II. FORMALISM

Following Ref. [28], it is useful to begin by recalling the essentials of the $B^+ \to DK^+$, $D \to K_S^0\pi^+\pi^-$ model-independent method [29–32]. The amplitude of the decay is written as a function of D decay Dalitz plot coordinates $(m_+^2, m_-^2) \equiv (m^2_{K_S^0\pi^+}, m^2_{K_S^0\pi^-})$,

$$A_{D\mathrm{Dlz}} = \bar{A}_D + r_B e^{i(\delta_B+\gamma)} A_D, \tag{1}$$

where $\bar{A}_D = \bar{A}_D(m_+^2, m_-^2)$ is the amplitude of the $\bar{D}^0 \to K_S^0\pi^+\pi^-$ decay, and $A_D = A_D(m_+^2, m_-^2)$ is the amplitude of the $D^0 \to K_S^0\pi^+\pi^-$ decay. (The favored B decay amplitude, which multiplies the right-hand side of Eq. (1), is conventionally omitted as it does not affect the observables of interest.) Assuming no CP violation in D decay, $A_D(m_+^2, m_-^2) = \bar{A}_D(m_-^2, m_+^2)$.[3] The density of the D decay Dalitz plot from $B^+ \to DK^+$ decay is then given by

$$|A_{D\mathrm{Dlz}}|^2 = |\bar{A}_D|^2 + r_B^2|A_D|^2 + 2|A_D||\bar{A}_D|(x_+c - y_+s), \tag{2}$$

[3]Effects due to CP violation in D decay are known to be sufficiently small that they can be neglected [6]. Charm mixing effects are more important, but it is well-known how to take them into account in the analysis [10,34–36], thus they are not considered in this paper. Effects due to CP violation in the $K^0\bar{K}^0$ system are also negligible [37].

where the functions $c = c(m_+^2, m_-^2)$ and $s = s(m_+^2, m_-^2)$ are the cosine and sine of the strong phase difference $\delta_D(m_+^2, m_-^2) = \arg A_D(m_+^2, m_-^2) - \arg \bar{A}_D(m_+^2, m_-^2)$ between the $D^0 \to K_S^0\pi^+\pi^-$ and $\bar{D}^0 \to K_S^0\pi^+\pi^-$ amplitudes. The parameters $x_\pm = r_B \cos(\delta_B \pm \gamma)$ and $y_\pm = r_B \sin(\delta_B \pm \gamma)$ are those defined in Sec. I. The equations for the charge-conjugate mode $B^- \to DK^-$ are obtained with the substitution $\gamma \to -\gamma$, i.e., $(x_+, y_+) \to (x_-, y_-)$, and $\bar{A}_D \leftrightarrow A_D$. Considering both B charges, one can obtain γ and δ_B separately.

Once the Dalitz plot is divided into $2\mathcal{N}$ bins symmetrically to the exchange $m_-^2 \leftrightarrow m_+^2$, the expected number of events in the i^{th} bin of the $D \to K_S^0\pi^+\pi^-$ Dalitz plot from $B^+ \to DK^+$ decay is

$$\langle N_i \rangle = h_{D\text{Dlz}}\Big[K_i + r_B^2 K_{-i} + 2\sqrt{K_i K_{-i}}(x_+ c_i - y_+ s_i)\Big], \tag{3}$$

where $h_{D\text{Dlz}}$ is a normalization constant. The bin index i ranges from $-\mathcal{N}$ to $\mathcal{N}$ (excluding 0); the exchange $m_+^2 \leftrightarrow m_-^2$ corresponds to the exchange $i \leftrightarrow -i$. The per-bin coefficients c_i and s_i are given by

$$c_i = \frac{\int_{\mathcal{D}_i} |A_D||\bar{A}_D| \cos\delta_D d\mathcal{D}}{\sqrt{\int_{\mathcal{D}_i} |A_D|^2 d\mathcal{D} \int_{\mathcal{D}_i} |\bar{A}_D|^2 d\mathcal{D}}},$$
$$s_i = \frac{\int_{\mathcal{D}_i} |A_D||\bar{A}_D| \sin\delta_D d\mathcal{D}}{\sqrt{\int_{\mathcal{D}_i} |A_D|^2 d\mathcal{D} \int_{\mathcal{D}_i} |\bar{A}_D|^2 d\mathcal{D}}}. \tag{4}$$

Here $\mathcal{D}$ represents the $D \to K_S^0\pi^+\pi^-$ Dalitz plot phase space and $\mathcal{D}_i$ is the bin region over which the integration is performed. The definitions of Eq. (4) imply the presence of a physical boundary, $c_i^2 + s_i^2 \le 1$.

Equation (3) also contains per-bin coefficients K_i, which can be obtained from the numbers of events in the corresponding bins of the Dalitz plot where the D meson is in a flavor eigenstate. Experimentally these can be obtained using $D^{*\pm} \to D\pi^\pm$ samples, where the charge of the emitted pion in the D^* decay tags the flavor of the D meson.

For $B^0 \to DK^+\pi^-$ decays, the variation of the amplitudes $\bar{A}_B$ for $B^0 \to \bar{D}^0 K^+\pi^-$ decay and A_B for $B^0 \to D^0 K^+\pi^-$ decay across the phase-space described by $(m_{D\pi}^2, m_{K\pi}^2)$ must be considered. For simplicity, the relative weak phase γ is factored out in the expressions that follow. The replacement for Eq. (1) is then

$$A_{\text{dbl Dlz}} = \bar{A}_B \bar{A}_D + e^{i\gamma} A_B A_D, \tag{5}$$

giving

$$|A_{\text{dbl Dlz}}|^2 = |\bar{A}_B|^2|\bar{A}_D|^2 + |A_B|^2|A_D|^2 + 2|\bar{A}_B||\bar{A}_D||A_B||A_D| \times [(\varkappa c - \sigma s)\cos\gamma - (\varkappa s + \sigma c)\sin\gamma], \tag{6}$$

where $\varkappa$ and σ are the cosine and sine of $\delta_B = \arg(A_B) - \arg(\bar{A}_B)$, and are functions of B decay Dalitz plot position. Then, after integrating over the phase-space of both the B and D decay Dalitz plot bins (with the former denoted by the index α, $1 \le \alpha \le \mathcal{M}$, and the latter by roman indices as before), the number of expected events in each bin is

$$\langle N_{\alpha i} \rangle = h_{\text{dbl Dlz}}\Big\{\bar{\kappa}_\alpha K_i + \kappa_\alpha K_{-i} + 2\sqrt{\kappa_\alpha K_i \bar{\kappa}_\alpha K_{-i}} \times [(\varkappa_\alpha c_i - \sigma_\alpha s_i)\cos\gamma - (\varkappa_\alpha s_i + \sigma_\alpha c_i)\sin\gamma]\Big\}, \tag{7}$$

where the B Dalitz plot bin phase terms are defined as

$$\varkappa_\alpha = \frac{\int_{\mathcal{D}_\alpha} |A_B||\bar{A}_B| \cos\delta_B d\mathcal{D}}{\sqrt{\int_{\mathcal{D}_\alpha} |A_B|^2 d\mathcal{D} \int_{\mathcal{D}_\alpha} |\bar{A}_B|^2 d\mathcal{D}}},$$
$$\sigma_\alpha = \frac{\int_{\mathcal{D}_\alpha} |A_B||\bar{A}_B| \sin\delta_B d\mathcal{D}}{\sqrt{\int_{\mathcal{D}_\alpha} |A_B|^2 d\mathcal{D} \int_{\mathcal{D}_\alpha} |\bar{A}_B|^2 d\mathcal{D}}}. \tag{8}$$

The true values of $\varkappa_\alpha$ and σ_α must satisfy $\varkappa_\alpha^2 + \sigma_\alpha^2 \le 1$. The corresponding expression to Eq. (7) for $\bar{B}^0 \to DK^-\pi^+$ decays is obtained with the substitution $\gamma \to -\gamma$.

The term $h_{\text{dbl Dlz}}$ that appears in Eq. (7) is a normalization constant. The factors $\bar{\kappa}_\alpha$ and κ_α are the B decay equivalents of the K_i factors for the D decay, but in this case there is no convenient independent control sample from which they can be obtained. Consequently, they must be determined as part of the analysis. Another important difference between the B and D Dalitz plots is that there is no symmetry inherent in the B decay since it is does not have a self-conjugate final state. This is reflected by the bin indices running from $1 \le \alpha \le \mathcal{M}$ for the B decay, in contrast to the choice $-\mathcal{N} \le i \le \mathcal{N}$ (excluding zero) for the D decay.

With $\mathcal{M}$ bins in the $B^0 \to DK^+\pi^-$ Dalitz plot and $2\mathcal{N}$ bins in the $D \to K_S^0\pi^+\pi^-$ Dalitz plot, then the number of equations represented by Eq. (7) and the charge-conjugate equivalent is $4\mathcal{M}\mathcal{N}$. For each of the $\mathcal{M}$ B decay Dalitz plot bins there are four unknown quantities to be determined: $\bar{\kappa}_\alpha$, κ_α, $\varkappa_\alpha$ and σ_α. Similarly, for each of the $\mathcal{N}$ D decay Dalitz plot bins there are factors of K_i, K_{-i}, c_i and s_i (after using $c_i = c_{-i}$ and $s_i = -s_{-i}$); however K_i, K_{-i} can be precisely determined from independent samples and c_i and s_i have been measured from $\psi(3770) \to D^0\bar{D}^0$ data [33]. Consequently, these should not be considered "unknown quantities," but can be allowed to vary within their uncertainties in the analysis. Finally, there are two global unknown parameters: the normalization factor h_{dblDlz} and γ. Thus, not counting the parameters associated with D decays, there are in total $4\mathcal{M} + 2$ quantities to be determined from the data.[4] Since typically $\mathcal{N} = 8$ is used for

[4]The discussion here differs from that in Ref. [28], where $\bar{\kappa}_\alpha$ and κ_α were considered to be independently known through the favored $D \to K^+\pi^-$ decay mode, and c_i and s_i were considered to be unknown.

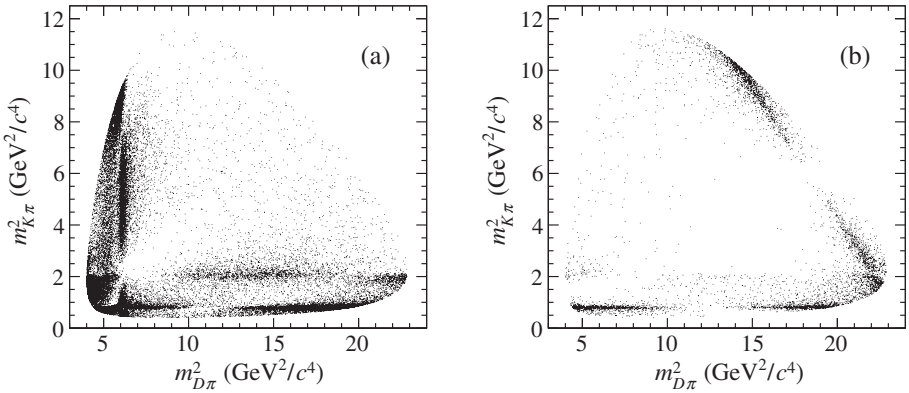

FIG. 1. Dalitz plot distributions obtained from the models used for the B decay amplitudes for the (left) favored amplitude, i.e., $B^0 \to \bar{D}^0 K^+\pi^-$, and (right) suppressed amplitude, i.e., $B^0 \to D^0 K^+\pi^-$. The former (latter) contains $D\pi^-$ (DK^+) resonances and does not contain DK^+ ($D\pi^-$) structures; both contain $K^+\pi^-$ resonances.

$D \to K^0_S\pi^+\pi^-$ decays, the system can in principle be solved for any value of $\mathcal{M}$.

The discussion above has been in the context of $D \to K^0_S\pi^+\pi^-$ decays, but is in fact valid, with appropriate choices of the hadronic parameters, for any D decay. Thus, for example, the $D \to K^0_S K^+K^-$ channel can be trivially included in the analysis: its inclusion is equivalent to simply adding more bins corresponding to different regions of D decay phase space, though in practice it will also be convenient to allow different normalization factors h for the different D decay modes. Inclusion of the two-body decays $D \to K^+K^-$ and $\pi^+\pi^-$ corresponds to a single bin with $c_i = 1$, $s_i = 0$ and $K_i = K_{-i}$ (in this case, the K factors can be conveniently absorbed into the normalization). For a CP-odd eigenstate one would have $c_i = -1$, $s_i = 0$, while for so-called quasi-CP-eigenstates c_i takes the value of the net CP content (discussion of quasi-CP-eigenstates can be found, for example, in Refs. [38–40]). The suppressed $D \to K^-\pi^+$ decay can be included with $K_i/K_{-i} = r^2_{K\pi}$, $c_i = \cos\delta_{K\pi}$ and $s_i = \sin\delta_{K\pi}$, while for the favored $D \to K^+\pi^-$ decay one should have instead $K_i/K_{-i} = r^{-2}_{K\pi}$, $c_i = \cos\delta_{K\pi}$ and $s_i = -\sin\delta_{K\pi}$. Here, $r_{K\pi} = 0.0590 \pm 0.0003$ and $\delta_{K\pi} = (15^{+8}_{-10})^\circ$ [6], are the relative magnitude and phase of the suppressed and favored D decay amplitudes to the $K^\pm\pi^\mp$ final states (note that care needs to be taken to ensure consistent phase conventions). Similar expressions can be used for multibody suppressed/favored pairs of modes such as $D \to K^\pm\pi^\mp\pi^0$ with the coherence factor included in the relations for c_i and s_i [21,39–41]. Relevant expressions for any other D decay modes can easily be obtained.

III. SENSITIVITY STUDY

In order to estimate the sensitivity of the method, simulated pseudoexperiments are generated and fitted. To generate the Dalitz plot distributions, the favored B decay amplitude corresponds to that in the LHCb publications [22,23], and the D Dalitz plot model is that from Ref. [42]. In the baseline model, the suppressed B decay amplitude is generated fixing the ratio of magnitudes of suppressed and favored amplitudes r_B to 0.3 for all of the $K^*(892)^0$, $K^*(1410)^0$, $K^*_2(1430)^0$ and $K\pi$ S-wave contributions, while taking the relative phases from the LHCb results [22]. The suppressed B decay amplitude also includes a $D^*_{s1}(2700)^+$ component at the level indicated by the results of Ref. [22]. Dalitz plot distributions obtained by generating with only the favored or suppressed B decay amplitude are shown in Fig. 1.

Samples sizes generated correspond roughly to the expected yields at LHCb after the completion of Run II and after accumulating 50 fb^{-1} of pp collision data at the end of the upgrade; these are given in Table I. The expected $B^0 \to DK^+\pi^-$ yields in the $D \to K^+\pi^-$, K^+K^- and $\pi^+\pi^-$ channels are extrapolated from those obtained in Run I [22].[5] The expected yield in the $D \to K^-\pi^+$ channel is obtained from the model assuming the same experimental efficiency, and hence normalization factor, as for the $D \to K^+\pi^-$ mode. In the $D \to K^0_S\pi^+\pi^-$ channel, the expected yields also include an extrapolation from the published Run I yields for $B^0 \to DK^{*0}$ [25,26] to the whole $B^0 \to DK^+\pi^-$ Dalitz plot.

The LHCb Run I data sample consists of 1 fb^{-1} collected at pp center-of-mass energy $\sqrt{s} = 7$ TeV and 2 fb^{-1} at $\sqrt{s} = 8$ TeV. The total Run II data sample is expected to include an additional 5 fb^{-1} collected at $\sqrt{s} = 13$ TeV, with the remainder of the 50 fb^{-1} sample expected to be collected at $\sqrt{s} = 14$ TeV and with trigger efficiency improved by around a factor of 2 [12]. The expected yields after Run II and after collecting 50 fb^{-1} are estimated accounting for the known variation of the production cross

[5]Reference [22] presents yields in the signal region in bins with varying background levels. The background-dominated bin has been excluded from the yields presented in Table I.

TABLE I. Samples sizes of $B^0 \to DK^+\pi^-$ decays in different D final states observed or expected, according to the baseline amplitude model, in the LHCb Run I data sample, with extrapolations to the samples that will be available after Run II and after collecting 50 fb^{-1}.

D decay mode	Run I	Run I + II	50 fb^{-1}
$K^+\pi^-$	2240	9200	140 000
$K^-\pi^+$	220	900	14 000
K^+K^-	270	1100	17 000
$\pi^+\pi^-$	130	540	8500
$K^0_S\pi^+\pi^-$	420	1700	27 000

section of B mesons within the LHCb acceptance up to $\sqrt{s} = 13$ TeV [43], and assuming linear scaling to 14 TeV.

It is of prime interest to investigate the optimal binning of the B decay Dalitz plot, though certain other variations of the conditions are also considered as discussed below. It has previously been shown [28,32] that optimizing a "binning quality factor" Q^2 leads to good sensitivity to γ. In the limit of zero background, Q^2 is related to the sensitivity to the interference term between suppressed and favored amplitudes in Eq. (5) and can be expressed as

$$Q^2 = \frac{\sum_\alpha \kappa_\alpha (\kappa_\alpha^2 + \sigma_\alpha^2)}{\sum_\alpha \kappa_\alpha}. \quad (9)$$

The binning that maximizes this expression for Q^2 is obtained by a stochastic optimization procedure described in detail in Ref. [33].

Schemes with different numbers of bins in the B decay Dalitz plot are considered. Examples of the binning obtained by maximizing Q^2 with the baseline amplitude model for $\mathcal{N} = 3$, 5, 8, 12, and 20 are shown in Fig. 2.

The $D \to K^0_S\pi^+\pi^-$ Dalitz plot is binned with $\mathcal{N} = 8$, which has become the de facto standard in the literature. The values of c_i and s_i are calculated from the D Dalitz plot amplitude model [42], and are consistent with those measured by the CLEO-c collaboration [33]. The effect on the sensitivity to γ from uncertainties on c_i and s_i is evaluated by considering cases where c_i and s_i are fixed (which is the baseline), where uncertainties from Ref. [33] are included as Gaussian constraints, and where c_i and s_i are freely floated in the fit. The values of K_i are assumed to be known with negligible uncertainty.

Only the D decays to $K^0_S\pi^+\pi^-$ and two-body final states are included in the study, since these are expected to be the most sensitive to γ, although other channels can be added as discussed in Sec. II. The suppressed $D \to K^-\pi^+$ channel is expected to be the most challenging experimentally, due to the large background from $B^0_s \to D^*K^-\pi^+$ decays. Therefore, the impact of including this channel or not in the analysis is investigated.

The purpose of the study is to investigate the potential sensitivity, and therefore experimental effects such as backgrounds and efficiency variations are not studied. An exception is made for the $B^0_s \to D^*K^-\pi^+$ background, which is expected to be particularly important for analyses at LHCb. Since the amplitude structure of this decay has not yet been studied, it is modelled with a cocktail of different resonant contributions: $D^*\bar{K}^{*0}$ (45%), $D_{s1}(2536)^-\pi^+$ (12%), $D^*_{s2}(2573)^-\pi^+$ (12%), $D^*_{s1}(2700)^-\pi^+$ (12%) and nonresonant $D^*K^-\pi^+$ decays (7%). A contribution from $B^0_s \to D_s(2650)^-\pi^+$ (12%) is also included, where the (unobserved) $D_s(2650)^-$ state is the radially excited pseudoscalar of the charm-strange meson spectrum. Each component of the $B^0_s \to D^*K^-\pi^+$ cocktail is generated using RapidSim [44] and EvtGen [45]. The distribution of the $DK\pi$ invariant mass for generated decays is shown in Fig. 3 along with distributions of the two-body invariant masses. The soft neutral particle from D^* decay is not included in the reconstruction of the candidate leading to a broad $DK\pi$ invariant mass distribution peaking near $m_{B^0_s} - (m_{D^{*0}} - m_{D^0}) \approx 5.2$ GeV/c^2, with a significant component within the B^0 signal region. Figure 4 shows the distribution of this simulated background in the $DK^-\pi^+$ Dalitz plot, for decays with $DK^-\pi^+$ invariant mass within ± 50 MeV/c^2 of the B^0 mass.

In addition to LHCb, large yields of the $B^0 \to DK^+\pi^-$ decay are also expected at the Belle II experiment, which is planned to collect 50 ab^{-1} of e^+e^- collision data. There is not sufficient information publicly available to make reliable estimates of the yields that can be obtained at Belle II, and therefore this is not attempted. Compared to LHCb, one might expect the relative yield of $D \to K^0_S\pi^+\pi^-$ compared to the two-body final states to be higher at Belle II, since a larger fraction of the K^0_S mesons decay within the region in which they are reconstructible. However, it is not clear from the published yields in studies of $B^0 \to DK^{*0}$ decays, with $D \to K^\mp\pi^-$ [46] and $K^0_S\pi^+\pi^-$ [47] whether this is realized in practice, as the effect of different selection requirements also impacts the relative yield. Another notable difference between LHCb and Belle II is that it is expected to be possible to include high-yield CP-odd channels such as $D \to K^0_S\pi^0$ in the Belle II analysis. A dedicated study would be necessary to investigate the potential sensitivity of this method with the Belle II data sample, but as a rough estimate it is expected that the precision should be around a factor of two worse than that of LHCb with 50 fb^{-1}, in the scenario without $B^0_s \to D^*K^-\pi^+$ background.

A. Dependence of the sensitivity to γ on the B Dalitz plot binning

Ensembles of pseudoexperiments are generated in an unbinned way, according to the B and D Dalitz plot models. The data in each pseudoexperiment are then binned according to a given scheme, and the yields in each bin are fitted to determine the following free parameters: the values of κ_α, $\bar{\kappa}_\alpha$ (which are effectively determined from the

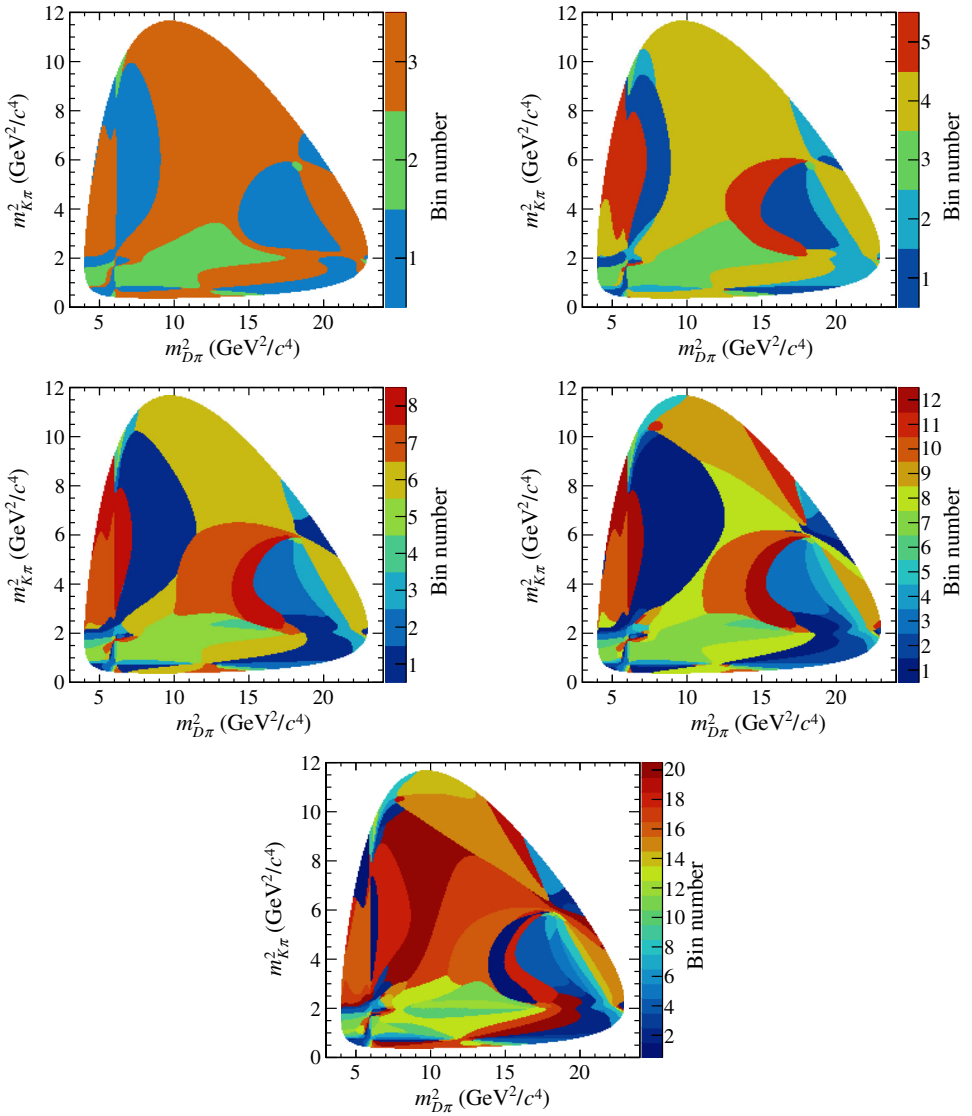

FIG. 2. Different B Dalitz plot binning schemes obtained by maximizing Q^2 with $\mathcal{N} = 3$, 5, 8, 12 and 20, as indicated by the z-axis.

favored $B^0 \to DK^+\pi^-$, $D \to K^+\pi^-$ sample), $\varkappa_\alpha$, σ_α, normalization factors for each channel and γ. The fit maximizes a likelihood obtained from Eq. (7) by allowing a Poisson distribution of the yield around the expected value in each bin. The values of $\varkappa_\alpha$ and σ_α are constrained to lie inside the physical region $\varkappa_\alpha^2 + \sigma_\alpha^2 \leq 1$; similarly $c_i^2 + s_i^2 \leq 1$ is imposed.[6] It may be noted from Eq. (7) that there could be potential benefit from fitting for $\cos\gamma$ and $\sin\gamma$ independently, but it appears that γ exhibits good statistical behavior as a free parameter of the fit, and as such it is simpler to handle it in this way. The expected uncertainty on γ is then obtained from the spread of values obtained from the fits to pseudoexperiments in the ensemble.

[6]These requirements are necessary to prevent the fit from predicting, through Eq. (7), negative yields in some bins leading to an unphysical likelihood function.

The results of the fits are shown in Figs. 5, 6 and 7. Figure 5 illustrates the effect of "optimal" binning compared to an alternative binning with uniform division of the strong phase difference between the $B^0 \to D^0K^+\pi^-$ and $B^0 \to \bar{D}^0K^+\pi^-$ amplitudes ("equal phase-difference" binning). The fits are performed to samples corresponding to the 50 fb^{-1} scenario with the baseline amplitude model. The result of the fit for each pseudoexperiment is represented by a colored point, where the color denotes the bin number α. It can be seen that the "optimal" binning results in $\varkappa_\alpha$, σ_α values that tend to be closer to the unit circle, corresponding to higher coherence in each of the bins and thus better sensitivity according to Eq. (9).

Figure 6 shows residual distributions for γ obtained from the fits, for each of the Run I + II and 50 fb^{-1} scenarios both with and without the suppressed $D \to K^-\pi^+$ mode included in the likelihood. Pseudoexperiments are generated with the

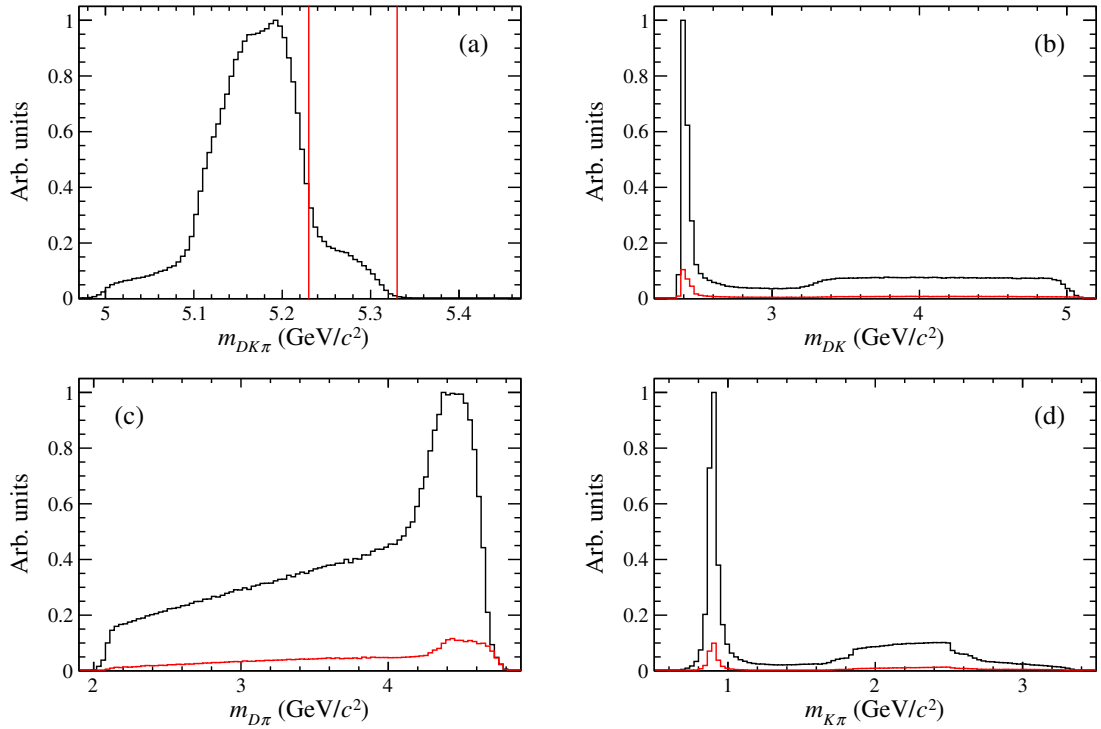

FIG. 3. Distribution of simulated $B_s^0 \to D^* K^- \pi^+$ decays in (top left—bottom right) $m(DK^-\pi^+)$, $m(DK^-)$, $m(D\pi^+)$ and $m(K^-\pi^+)$. Red histograms show the distribution of decays with $DK^-\pi^+$ mass within ± 50 MeV/c^2 of the B^0 mass, indicated by vertical red lines on the $m(DK^-\pi^+)$ distribution.

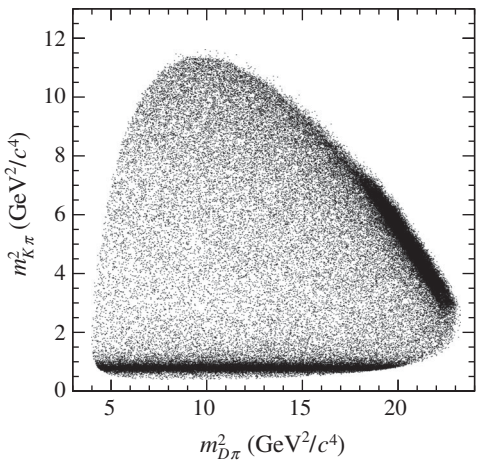

FIG. 4. Distribution of simulated $B_s^0 \to D^* K^- \pi^+$ decays in the $DK^-\pi^+$ Dalitz plot for decays with $DK^-\pi^+$ invariant mass within ± 50 MeV/c^2 of the B^0 mass.

baseline model and the fits are performed with the "optimal" binning with $\mathcal{M} = 12$. In all cases there is no visible bias in γ. The absence of significant bias is also verified for all binning schemes used in subsequent fits, with $\mathcal{M} = 3$, 5, 8, 12, and 20.

The resolution of γ obtained from fits to the residual distributions as a function of the number of bins $\mathcal{M}$ for both "equal phase-difference" and "optimal" binning schemes, with and without the $D \to K^+\pi^-$ mode in the likelihood, are shown in Fig. 7. Overall, removing the $D \to K^+\pi^-$ mode results in only 3–10% increase in the uncertainty on γ. The use of "optimal" binning results in consistently better resolution than with the "equal phase-difference" binning for sufficiently large number of bins ($\mathcal{M} > 5$). Therefore, "optimal" binning schemes are used for all subsequent studies.

B. Dependence on the uncertainty of the c_i and s_i factors

As discussed in Sec. II, the coefficients c_i and s_i have been measured and are therefore not considered as unknown parameters. In the baseline analysis, all c_i and s_i are fixed to their known true values as predicted by the D decay amplitude model. In an experimental analysis one would instead use the measured central values [33], and the values of c_i and s_i could be varied within their uncertainties to evaluate the associated systematic uncertainty. However, the $B^0 \to DK^-\pi^+$ double Dalitz plot analysis itself also provides sensitivity to c_i and s_i, owing to the large value of the interference term. A natural approach is therefore to include the externally measured values of c_i and s_i into the likelihood with Gaussian constraints. In this way, the uncertainty in the external determination of c_i and s_i enters the statistical uncertainty of the result. Alternatively, the c_i and s_i

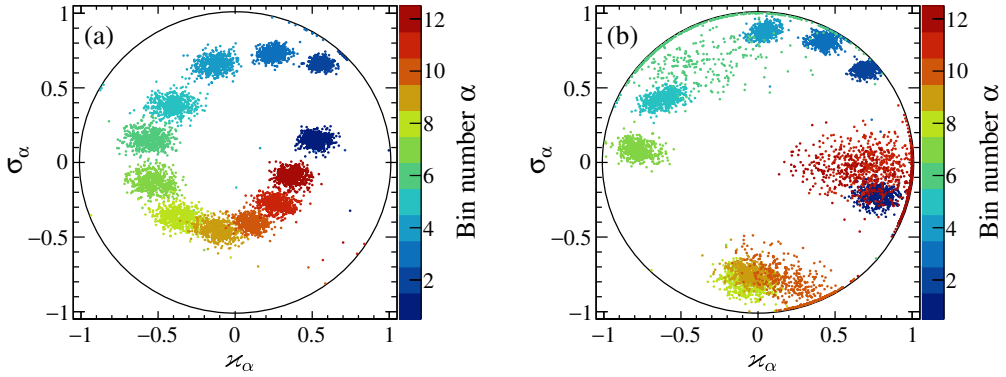

FIG. 5. Fitted $\varkappa_\alpha$ and σ_α values for the 50 fb^{-1} scenario with (a) "equal phase-difference" and (b) "optimal" binning schemes.

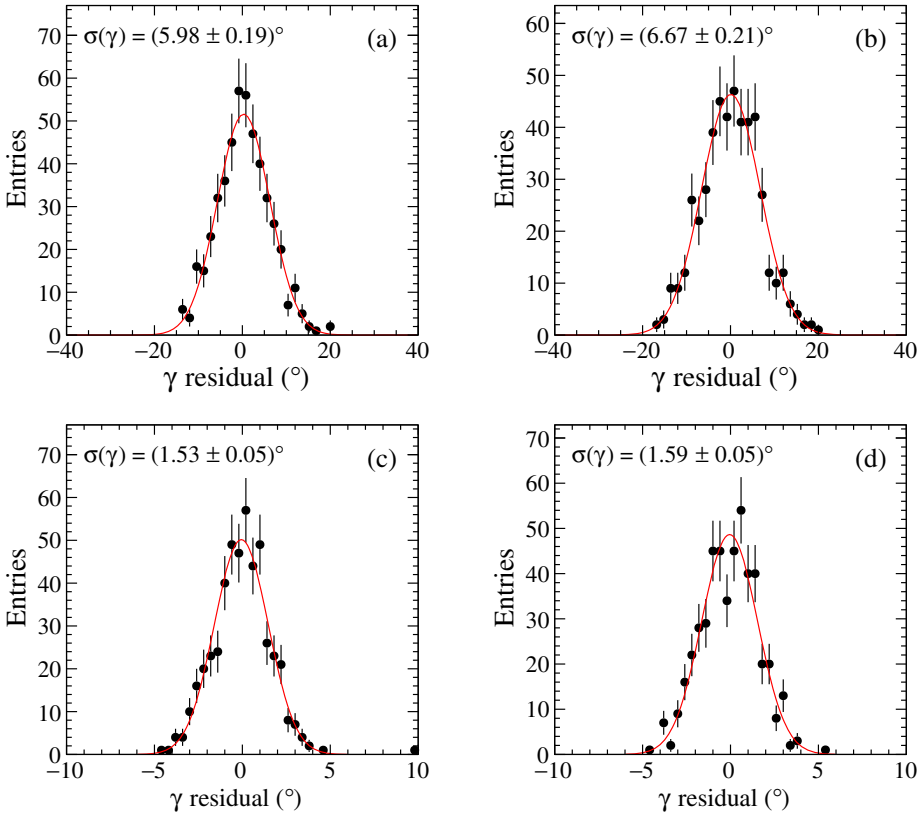

FIG. 6. Residual distributions for γ for the (a,b) Run I + II and (c,d) 50 fb^{-1} scenarios (a,c) with and (b,d) without the $D^0 \to K^+\pi^-$ mode. The solid lines show the results of Gaussian fits to the distributions.

parameters can be treated as unknown and floated in the fit, removing the dependence on external measurements.

The impact of these different approaches to external constraints on c_i and s_i is illustrated in Fig. 8, which shows the resolution on γ as a function of the number of bins $\mathcal{M}$ for the cases when c_i and s_i terms are fixed to their true values, when Gaussian constraints are applied corresponding to the current measurement uncertainties [33], and when c_i and s_i are left unconstrained. The difference between the extreme cases of fixing or floating the c_i and s_i parameters is quite significant for the Run I + II scenario, particularly for smaller $\mathcal{M}$. However, the precision of the current measurements of c_i and s_i appears to be sufficient so that the sensitivity to γ is not degraded substantially. Interestingly, as the data sample increases, the importance of precise external measurements of c_i and s_i reduces, in contrast to the situation for the model-independent analysis of $B^+ \to DK^+$ with $D \to K^0_S\pi^+\pi^-$ decays [48], as the double Dalitz plot analysis itself constrains these parameters. Figure 9 shows as an example the fitted values of the c_i and s_i parameters from fits in the 50 fb^{-1} scenario; the uncertainties are in the range 0.07–0.17,

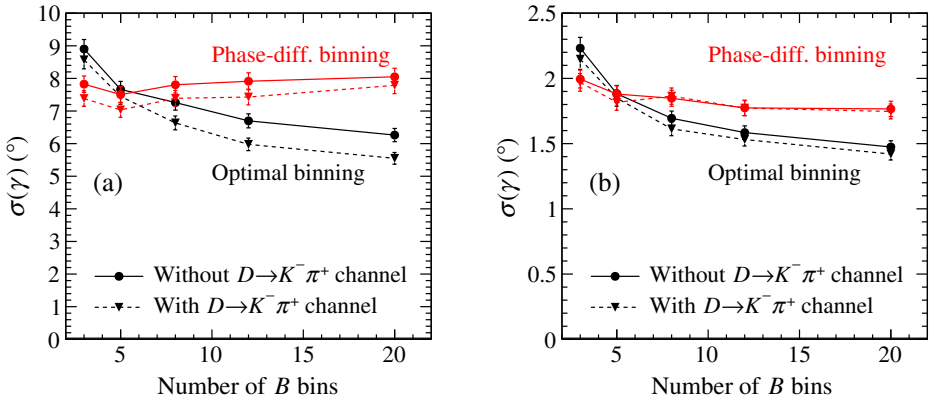

FIG. 7. Sensitivity to γ obtained with yields in each channel according to the (a) Run I + II and (b) 50 fb^{-1} scenarios. Results are shown for both "equal phase-difference" and "optimal" binning schemes. The lines joining the points are added simply to guide the eye.

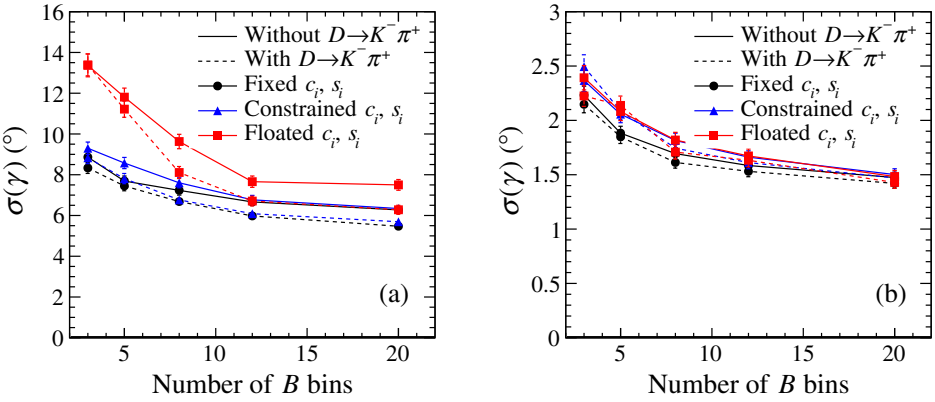

FIG. 8. Impact of the uncertainty on the c_i and s_i parameters on the sensitivity to γ for the (a) Run I + II and (b) 50 fb^{-1} scenarios. Results are shown with c_i, s_i values fixed to their true values, constrained within the precision of the current measurements [33], and left free to float in the fit. The lines joining the points are added simply to guide the eye.

comparable to or somewhat better than those of the current measurements [33]. Nonetheless, precise independent external measurements of c_i and s_i, as could be obtained by the BESIII experiment, would remain important to provide a cross-check of the measurement.

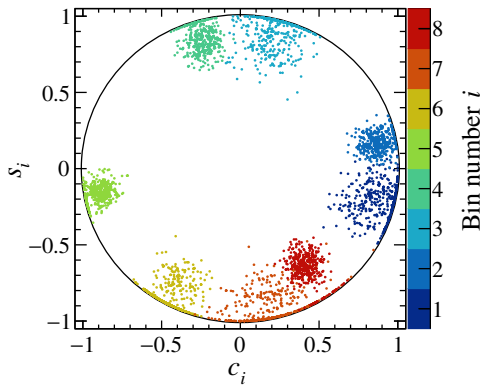

FIG. 9. Fitted c_i and s_i values for the 50 fb^{-1} scenario with $\mathcal{M} = 8$ and no external constraints.

C. Dependence on the value of r_B

The sensitivity to γ is expected to have a strong dependence on the ratio of magnitudes of the suppressed and favored amplitudes. For (quasi-)two-body decays, this ratio is quantified by the value r_B, which can differ for each kaonic state produced in a $B \to DK$-type process. In the baseline model, $r_B = 0.3$ is used for all of the $K^*(892)^0$, $K^*(1410)^0$, $K_2^*(1430)^0$ and $K\pi$ S-wave contributions. The effect of varying r_B to smaller or larger values is shown in Fig. 10. As expected, larger values of r_B result in better sensitivity. It can also be noted that the impact of the $D \to K^-\pi^+$ channel is more significant for smaller values of r_B.

D. Effect of $B_s^0 \to D^*K^-\pi^+$ background

Based on the yield of the $B_s^0 \to D^*K^-\pi^+$ background in Ref. [22], the expected level of this background relative to signal in the modes $B^0 \to DK^-\pi^+$ with $D \to K^+K^-$, $\pi^+\pi^-$ and $K_S^0\pi^+\pi^-$ is around 20% in the ± 35 MeV/c^2 region around the B meson mass. For the suppressed mode with $D \to K^-\pi^+$, however, the background-to-signal ratio is expected to be around 7.5. This mode is therefore

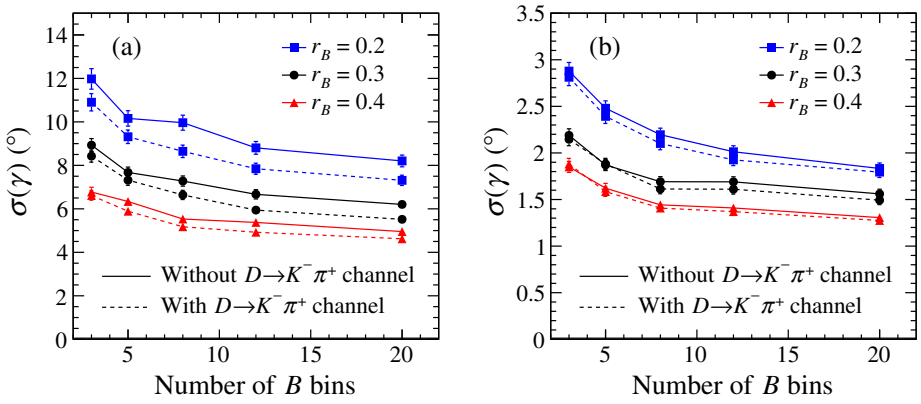

FIG. 10. Sensitivity to γ in the (a) "Run I+II" and (b) "50 fb^{-1}" scenarios, as a function of number of bins used for the B Dalitz plot, shown for $r_B = 0.2$ (blue), 0.3 (black) and 0.4 (red). The lines joining the points are added simply to guide the eye.

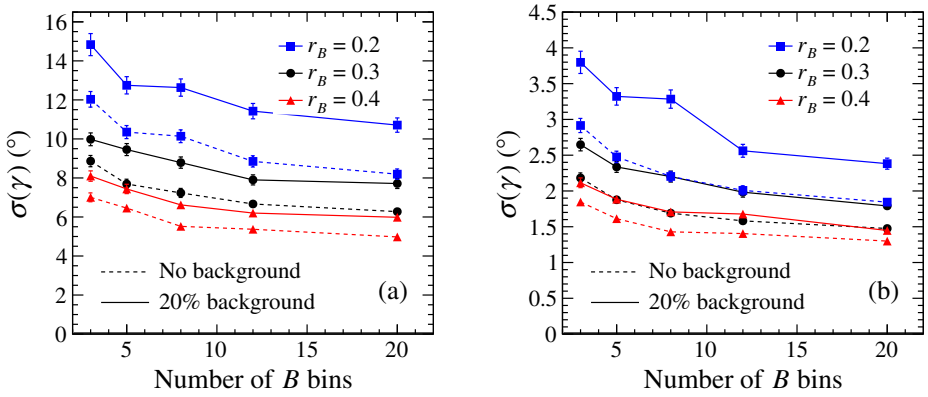

FIG. 11. Sensitivity to γ in the (a) "Run I+II" and (b) "50 fb^{-1}" scenarios, as a function of number of bins of the B Dalitz plot, shown for $r_B = 0.2$ (blue), 0.3 (black) and 0.4 (red), without background (dashed line) and with the expected amount of $B^0_s \to D^*K^-\pi^+$ background (solid line). The lines joining the points are added simply to guide the eye. Note that the points with no background correspond to those in Fig. 10 without the $D \to K^-\pi^+$ channel.

considered to be background-dominated and is not considered in the background-enabled fits.

The expected background yields $\langle N^{(\mathrm{bck})}_{\alpha i}\rangle$ ($\langle N^{(\mathrm{bck})}_{\alpha}\rangle$) are calculated for each B bin α and D bin i for the $D \to K^0_S\pi^+\pi^-$ mode (for each B bin α for two-body D decays) according to the expected Dalitz plot distribution (Figs. 3 and 4) and assuming that the D meson is produced purely by the $b \to c$ transition. A random amount of background $N^{(\mathrm{bck})}_{\alpha(i)}$ is generated according to a Poisson distribution with mean $\langle N^{(\mathrm{bck})}_{\alpha(i)}\rangle$ and is added to the signal yield. The expected background yields are then accounted for in the Poisson terms for each bin entering the likelihood function used in the fit to determine γ.

The comparison of the sensitivity to γ with and without the $B^0_s \to D^*K^-\pi^+$ background included is shown in Fig. 11. A deterioration in precision is seen in all scenarios, although the effect is larger for smaller values of r_B. The size of the effect, around 10%, is significant but not large enough to threaten the viability of the method. It may be possible to ameliorate the impact in an experimental analysis through selection requirements that discriminate against $B^0_s \to D^*K^-\pi^+$ background or by taking the presence of the background into account in the determination of the binning scheme [32,33].

E. Impact of mismodeling of the B decay amplitudes

While the optimal binning of the B decay phase space depends on the model, the measurement is unbiased even if the model used to define the binning differs from the true amplitude. However, the statistical uncertainty of the measurement might be affected by mismodeling. This effect is investigated by using alternative models for the binning optimization with Eq. (9), while the pseudoexperiments are always generated according to the baseline model.

It is expected that most aspects of the favored $b \to c$ amplitude will be well known from the favored mode, therefore most of the model variations considered relate to the suppressed amplitude only. These include removing the $D^*_s(2700)$ state, as well as using $r_B = 0.2$ or 0.4 instead of

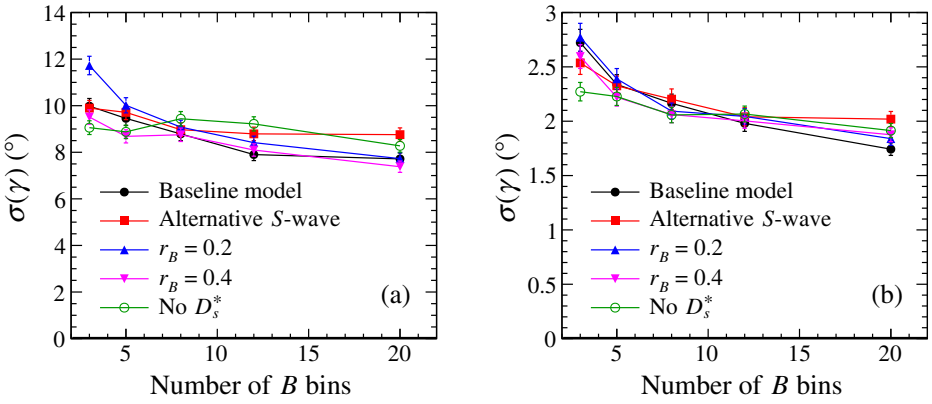

FIG. 12. Sensitivity to γ in the (a) "Run I+II" and (b) "50 fb^{-1}" scenarios, as a function of number of bins of the B Dalitz plot, with different B^0 decay models used for binning optimization. The lines joining the points are added simply to guide the eye.

the baseline $r_B = 0.3$. There is also uncertainty related to the modeling of the broad $K\pi$ and $D\pi S$-wave components (for the former appearing in both favored and suppressed amplitudes; for the latter only in the favored mode). The impact of using alternative S-wave line shapes in the binning optimization to those in the generation is therefore considered, in a similar way to Ref. [22]. The results of this study are shown in Fig. 12. Event samples are generated with the baseline model and with $B_s^0 \to D^* K^- \pi^+$ background included at the expected level. The possible impact on the sensitivity to γ is at the level of 10%, which is considered sufficiently small not to be a major concern.

IV. SUMMARY

The model-independent double Dalitz plot analysis of $B^0 \to DK^-\pi^+$ with, at least, $D \to K^0_S\pi^+\pi^-$ decays provides an attractive approach to the measurement of the angle γ of the CKM unitarity triangle. Using recently published information on the favored and suppressed B decay amplitudes [22,23], the potential sensitivity of the method has been examined. It is seen that sensitivities of around 8° and 2° can be expected for LHCb data samples corresponding to the expected amount of data collected at the end of the LHC Run II and after 50 fb^{-1} have been collected. These values are only around a factor of two larger than those expected from the combination of many results from LHCb [12], demonstrating that this method can have a significant impact. The sensitivity depends strongly on the ratio of magnitudes of suppressed and favored B decay amplitudes, which is not yet well known. The dependence on the choice of model for the binning and the impact of background have been shown to be modest. Thus, the major sources of systematic uncertainty that affect the determination of γ from amplitude analysis of $B^0 \to DK^+\pi^-$ decays [22] are much less significant in the model-independent double Dalitz plot approach. The method does not depend strongly on external constraints on the hadronic parameters c_i and s_i associated with the $D \to K^0_S\pi^+\pi^-$ decay, in contrast to the model-independent analysis for $B^+ \to DK^+$ with multibody D decays. The double Dalitz plot approach is expected also to be relevant for the Belle II experiment, where there will be no background from $B_s^0 \to D^* K^- \pi^+$ decays. Further improvement in sensitivity may be achieved by optimizing the binning taking backgrounds into account, or by adding further D decay modes to the analysis, using the formalism set out in this paper.

ACKNOWLEDGMENTS

The authors wish to thank their colleagues on the LHCb experiment for the fruitful and enjoyable collaboration that inspired this study. In particular, they would like to thank Matt Kenzie, Dan Johnson and Mark Whitehead for helpful comments on the manuscript. This work is supported by the Science and Technology Facilities Council and by the English-Speaking Union (United Kingdom).

[1] N. Cabibbo, Unitary Symmetry and Leptonic Decays, Phys. Rev. Lett. **10**, 531 (1963).

[2] M. Kobayashi and T. Maskawa, *CP* violation in the renormalizable theory of weak interaction, Prog. Theor. Phys. **49**, 652 (1973).

[3] C. Jarlskog, Commutator of the Quark Mass Matrices in the Standard Electroweak Model and a Measure of Maximal *CP* Violation, Phys. Rev. Lett. **55**, 1039 (1985).

[4] J. Brod and J. Zupan, The ultimate theoretical error on γ from $B \to DK$ decays, J. High Energy Phys. 01 (2014) 051.

[5] J. Brod, A. Lenz, G. Tetlalmatzi-Xolocotzi, and M. Wiebusch, New physics effects in tree-level decays and the precision in the determination of the quark mixing angle γ, Phys. Rev. D **92**, 033002 (2015).

[6] Y. Amhis *et al.* (Heavy Flavor Averaging Group), Averages of b-hadron, c-hadron, and τ-lepton properties as of summer 2016, Eur. Phys. J. C **77**, 895 (2017).

[7] R. Aaij *et al.* (LHCb collaboration), Measurement of *CP* observables in $B^\pm \to DK^\pm$ and $B^\pm \to D\pi^\pm$ with two- and four-body D decays, Phys. Lett. B **760**, 117 (2016).

[8] R. Aaij *et al.* (LHCb collaboration), Measurement of the CKM angle γ using $B^\pm \to DK^\pm$ with $D \to K^0_S\pi^+\pi^-$, $K^0_S K^+K^-$ decays, J. High Energy Phys. 10 (2014) 097.

[9] R. Aaij *et al.* (LHCb collaboration), Measurement of *CP* observables in $B^\pm \to D^{(*)}K^\pm$ and $B^\pm \to D^{(*)}\pi^\pm$ with $D^0 \to K\pi$, KK, $\pi\pi$ decays, Phys. Lett. B **777**, 16 (2018).

[10] R. Aaij *et al.* (LHCb collaboration), Measurement of the CKM angle γ from a combination of LHCb results, J. High Energy Phys. 12 (2016) 087.

[11] LHCb Collaboration, Report No. LHCb-CONF-2017-004.

[12] R. Aaij, A. Bharucha *et al.* (LHCb collaboration), Implications of LHCb measurements and future prospects, Eur. Phys. J. C **73**, 2373 (2013).

[13] R. Aaij *et al.* (LHCb collaboration), Report No. CERN-LHCC-2017-003, 2017.

[14] T. Aushev *et al.*, Physics at super B factory, arXiv: 1002.5012; Report No. KEK-REPORT-2009-12.

[15] T. Gershon and V. V. Gligorov, *CP* violation in the B system, Rept. Prog. Phys. **80**, 046201 (2017).

[16] T. Gershon, On the measurement of the unitarity triangle angle γ from $B^0 \to DK^{*0}$ decays, Phys. Rev. D **79**, 051301 (2009).

[17] T. Gershon and M. Williams, Prospects for the measurement of the unitarity triangle angle γ from $B^0 \to DK^+\pi^-$ decays, Phys. Rev. D **80**, 092002 (2009).

[18] M. Gronau and D. London, How to determine all the angles of the unitarity triangle from $B^0 \to DK^0_S$ and $B^0_s \to D\phi$, Phys. Lett. B **253**, 483 (1991).

[19] M. Gronau and D. Wyler, On determining a weak phase from *CP* asymmetries in charged B decays, Phys. Lett. B **265**, 172 (1991).

[20] D. Atwood, I. Dunietz, and A. Soni, Enhanced *CP* Violation with $B \to KD^0(\bar{D}^0)$ Modes and Extraction of the CKM Angle γ, Phys. Rev. Lett. **78**, 3257 (1997).

[21] D. Atwood, I. Dunietz, and A. Soni, Improved methods for observing *CP* violation in $B^\pm \to KD$ and measuring the CKM phase γ, Phys. Rev. D **63**, 036005 (2001).

[22] R. Aaij *et al.* (LHCb collaboration), Constraints on the unitarity triangle angle γ from Dalitz plot analysis of $B^0 \to DK^+\pi^-$ decays, Phys. Rev. D **93**, 112018 (2016).

[23] R. Aaij *et al.* (LHCb collaboration), Amplitude analysis of $B^0 \to \bar{D}^0 K^+\pi^-$ decays, Phys. Rev. D **92**, 012012 (2015).

[24] T. Gershon (LHCb collaboration), Current challenges and future prospects for γ from $B \to Dhh'$ decays, *Proc. Sci.*, CKM2016 (2017) 115, [arXiv:1702.01535].

[25] R. Aaij *et al.* (LHCb collaboration), Model-independent measurement of the CKM angle γ using $B^0 \to DK^{*0}$ decays with $D \to K^0_S\pi^+\pi^-$ and $K^0_S K^+K^-$, J. High Energy Phys. 06 (2016) 131.

[26] R. Aaij *et al.* (LHCb collaboration), Measurement of the CKM angle γ using $B^0 \to DK^{*0}$ with $D \to K^0_S\pi^+\pi^-$ decays, J. High Energy Phys. 08 (2016) 137.

[27] M. Gronau, Improving bounds on gamma in $B^\pm \to DK^\pm$ and $B^{\pm,0} \to DX_s^{\pm,0}$, Phys. Lett. B **557**, 198 (2003).

[28] T. Gershon and A. Poluektov, Double Dalitz plot analysis of the decay $B^0 \to DK^+\pi^-$, $D \to K^0_S\pi^+\pi^-$, Phys. Rev. D **81**, 014025 (2010).

[29] A. Giri, Y. Grossman, A. Soffer, and J. Zupan, Determining γ using $B^\pm \to DK^\pm$ with multibody D decays, Phys. Rev. D **68**, 054018 (2003).

[30] A. Bondar, in *Proceedings of BINP special analysis meeting on Dalitz analysis, 24-26 Sep. 2002* (unpublished).

[31] A. Bondar and A. Poluektov, Feasibility study of model-independent approach to ϕ_3 measurement using Dalitz plot analysis, Eur. Phys. J. C **47**, 347 (2006).

[32] A. Bondar and A. Poluektov, The use of quantum-correlated D^0 decays for ϕ_3 measurement, Eur. Phys. J. C **55**, 51 (2008).

[33] J. Libby *et al.* (CLEO collaboration), Model-independent determination of the strong-phase difference between D^0 and $\bar{D}^0 \to K^0_{S,L}h^+h^-$ ($h = \pi$, K) and its impact on the measurement of the CKM angle γ/ϕ_3, Phys. Rev. D **82**, 112006 (2010).

[34] J. P. Silva and A. Soffer, Impact of D^0–$\bar{D}^0$ mixing on the experimental determination of γ, Phys. Rev. D **61**, 112001 (2000).

[35] M. Rama, Effect of D^0–$\bar{D}^0$ mixing in the extraction of γ with $B^- \to D^0K^-$ and $B^- \to D^0\pi^-$ decays, Phys. Rev. D **89**, 014021 (2014).

[36] R. Aaij *et al.* (LHCb collaboration), A measurement of the CKM angle γ from a combination of $B^\pm \to Dh^\pm$ analyses, Phys. Lett. B **726**, 151 (2013).

[37] Y. Grossman and M. Savastio, Effects of $K^0\bar{K}^0$ mixing on determining γ from $B^\pm \to DK^\pm$, J. High Energy Phys. 03 (2014) 008.

[38] M. Nayak, J. Libby, S. Malde, C. Thomas, G. Wilkinson, R. A. Briere, P. Naik, T. Gershon, and G. Bonvicini, First determination of the *CP* content of $D \to \pi^+\pi^-\pi^0$ and $D \to K^+K^-\pi^0$, Phys. Lett. B **740**, 1 (2015).

[39] R. Aaij *et al.* (LHCb collaboration), A study of *CP* violation in $B^\mp \to Dh^\mp$ ($h = K$, π) with the modes $D \to K^\mp\pi^\pm\pi^0$, $D \to \pi^+\pi^-\pi^0$ and $D \to K^+K^-\pi^0$, Phys. Rev. D **91**, 112014 (2015).

[40] T. Gershon, J. Libby, and G. Wilkinson, Contributions to the width difference in the neutral D system from hadronic decays, Phys. Lett. B **750**, 338 (2015).

[41] N. Lowrey *et al.* (CLEO collaboration), Determination of the $D^0 \to K^-\pi^+\pi^0$ and $D^0 \to K^-\pi^+\pi^+\pi^-$ coherence factors and average strong-phase differences using quantum-correlated measurements, Phys. Rev. D **80**, 031105 (2009).

[42] A. Poluektov *et al.* (Belle collaboration), Evidence for direct CP violation in the decay $B \to D^{(*)}K$, $D \to K^0_S\pi^+\pi^-$ and measurement of the CKM phase ϕ_3, Phys. Rev. D **81**, 112002 (2010).

[43] R. Aaij *et al.* (LHCb collaboration), Measurement of forward J/ψ production cross-sections in pp collisions at $\sqrt{s} = 13$ TeV, J. High Energy Phys. 10 (2015) 172; Erratum, J. High Energy Phys. 05 (2017) 63.

[44] G. A. Cowan, D. C. Craik, and M. D. Needham, RapidSim: An application for the fast simulation of heavy-quark hadron decays, Comput. Phys. Commun. **214**, 239 (2017).

[45] D. J. Lange, The EvtGen particle decay simulation package, Nucl. Instrum. Methods Phys. Res., Sect. A **462**, 152 (2001).

[46] K. Negishi *et al.* (Belle collaboration), Search for the decay $B^0 \to DK^{*0}$ followed by $D \to K^-\pi^+$, Phys. Rev. D **86**, 011101 (2012).

[47] K. Negishi *et al.* (Belle collaboration), First model-independent Dalitz analysis of $B^0 \to DK^{*0}$, $D \to K^0_S\pi^+\pi^-$ decay, Prog. Theor. Exp. Phys. **2016**, 043C01 (2016).

[48] S. Malde *et al.* (LHCb collaboration), Report No. LHCb-PUB-2016-025.